UKRAINIAN JOURNAL OF MECHANICAL ENGINEERING AND MATERIALS SCIENCE

Vol. 7, No. 3–4, 2021

Vitaliy Korendiy

Department of Robotics and Integrated Mechanical Engineering Technologies, Lviv Polytechnic National University, 12, S. Bandery Str., Lviv, Ukraine, e-mail: vitaliy.nulp@gmail.com, ORCID 0000-0002-6025-3013

GENERALIZED DESIGN DIAGRAM AND MATHEMATICAL MODEL OF SUSPENSION SYSTEM OF VIBRATION-DRIVEN ROBOT

Received: June 28, 2021 / Revised: August 26, 2021 / Accepted: December 28, 2021

https://doi.org/10.23939/ujmems2021.03-04.001

Abstract. *Problem statement.* Mobile robotic systems are widely used in various fields of industry and social life: from small household appliances to large-size road-building machinery. Specific attention of scientists and designers is paid to the vibration-driven locomotion systems able to move in the environments where the use of classical wheeled and caterpillar robots is impossible or inefficient. *Purpose.* The main objective of this paper consists in generalizing the actual research results dedicated to various design diagrams and mathematical models of suspension systems of mobile vibration-driven robots. *Methodology.* The differential equations describing the robot motion are derived using the Lagrange-d'Alembert principle. The numerical modeling is carried out in the Mathematica software by solving the derived system of differential equations with the help of the Runge-Kutta methods. The verification of the obtained results is performed by computer simulation of the robot motion in the SolidWorks and MapleSim software. *Findings (results).* The time dependencies of the basic kinematic parameters (displacement, velocity, acceleration) of the robot's vibratory system are analyzed. The possibilities of maximizing the robot translational velocity are considered. *Originality (novelty).* The paper generalizes the existent designs and mathematical models of the mobile vibration-driven robots' suspensions and studies the combined four-spring locomotion system moving along a rough horizontal surface. *Practical value.* The obtained results can be effectively used by researchers and designers of vibration-driven locomotion systems while improving the existent designs and developing the new ones. *Scopes of further investigations.* While carrying out further investigations on the subject of the paper, it is necessary to solve the problem of optimizing the robot's oscillatory system parameters in order to maximize its translational velocity.

Keywords: mobile robotic system, locomotion system, numerical modelling, computer simulation, kinematic parameters, translational velocity, optimization problem.

Introduction and Problem Statement

Mobile robots are currently of significant interest among researcher in various fields of industry and social life [1]. The possibilities of practical implementation of classical wheeled and caterpillar drives are sometimes inexpedient or inefficient. Therefore, the specific attention of scientists and designers is paid to the vibration-driven locomotion systems considered as one of the most prospective drives of mobile robots [2]. In particular, the vibration-driven systems are usually used for cleaning and inspecting the internal surfaces of pipelines [3], in conveying equipment of mining industry [4], or in compacting machines used in the field of road-building [5]. There exist a number of developed designs of vibration-driven locomotion system that can be implemented in household appliances [6], agriculture [7], and medicine [8, 9].

The problems of studying the dynamic behavior of various designs of mobile vibration-driven systems are of significant interest among researchers all over the world. There exist a great variety of the robot's structures differing in the driving system, excitation mechanism, suspension, number of oscillating masses, etc. The vibration-driven locomotion systems are sometimes designed on the basis of the multi-module structures with several independent drives [2, 10, 11]. The operation of such systems is often based

on the vibro-impact excitation conditions [3, 8, 9, 12, 13]. Among a great variety of vibration exciters, the centrifugal ([2, 4, 5, 10]), electromagnetic ([3, 9, 12, 13]), and crank-type (eccentric) ([14, 15]) ones are the most widely used in mobile vibration-driven locomotion systems.

The specific attention of researchers is currently paid to the mobile robots equipped with bristles [16–18]. In particular, the paper [16] presents the numerical modelling and experimental investigation results describing the dynamic behavior of the mobile vibration-driven robot with bristle-type suspension lying on the vibrating surface. Similar theoretical and experimental research on locomotion conditions of the relatively small bristle-robot driven by a piezoelectric actuator was carried out in [17]. The paper [18] is devoted to designing and investigating the novel hybrid soft actuator for mobile robotic systems characterized by the controllable leaning direction of the elastic spikes.

Considering all the information sources mentioned above, the present paper is aimed at generalizing the actual research results dedicated to various design diagrams and mathematical models of suspension systems of mobile vibration-driven robots. The original idea of this study consists in developing and investigating the combined four-spring suspension of the self-propelled locomotion system moving along a rough horizontal surface and vibrationally excited by the generalized periodic forces. While carrying out the numerical modeling and computer simulation of the robot motion conditions, the applied software Mathematica [19], MapleSim [20], and SolidWorks [21] is to be used. This allows for carrying out the virtual experimental studies with no need to implement the robot's suspension in practice and verifying the correctness of the derived differential equations describing the robot motion.

Main Material Presentation

Generalized dynamic diagram of the robot's suspension system.

Based on the thorough analysis of numerous scientific papers related with vibration-driven robots' suspensions, the generalized dynamic diagram of the combined four-spring locomotion system moving along a rough horizontal surface is presented in Fig. 1. The rigid body 1 of the mass m_1 simulating the robot's working member is supported by the suspension system 2 and feet 3 on the horizontal surface 4. The suspension system 2 is based on two legs with two hinged spring-damper elements characterized by the corresponding stiffness (k_1, k_2) and damping (c_1, c_2) coefficients (see Fig. 1). The whole mass m_1 of the robot's body is concentrated at the point O, to which two independent perpendicularly directed forces $\boldsymbol{F}_{1x}$, $\boldsymbol{F}_{1y}$ are applied. Let us consider the case, when one force ($\boldsymbol{F}_{1x}$) is directed horizontally to the right, while the other one ($\boldsymbol{F}_{1y}$) acts vertically upwards. The applied assumption allows for studying the plane translational motion of the robot's body with no need to consider its angular inclination. The surface roughness is considered by applying the corresponding dry friction forces between the robot's feet and the supporting surface characterized by the static and kinematic friction coefficients $\mu_{fr.s}$, $\mu_{fr.k}$.

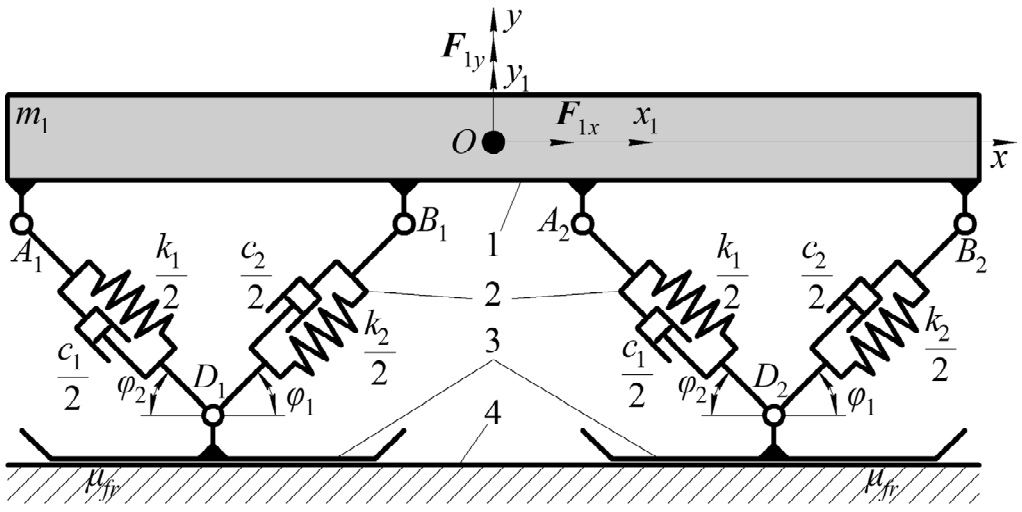

Fig. 1. Generalized dynamic diagram of the robot's suspension system

Let us apply the inertial Cartesian coordinate system *xOy* with its origin *O* located at the mass center of the robot's body in its equilibrium position (in the state of rest). The applied coordinate system is fixed to the unmovable supporting surface. The *Ox* axis is directed horizontally to the right and is parallel to the surface, while the *Oy* axis is directed vertically upwards. The angular positions of the straight lines connecting the hinges D_1, B_1 and D_1, A_1 are defined by the angles φ_1, φ_2, respectively. In general, the robot motion is characterized by two independent coordinates x_1, y_1 unambiguously describing the position of the robot's body mass center in the applied coordinate system *xOy* at each moment of time.

Mathematical model describing the system motion.

In order to derive the differential equations of the robot motion, let us use the Lagrange-d'Alembert principle. Among lots of statements of this principle, let use the following one: the mechanical system consisting of rigid bodies remains in the dynamic equilibrium when the total virtual work (the sum of the virtual works of the applied forces (active forces, reactions of constraints) and the inertial forces) is equal to zero for any virtual displacement of the considered system. In our case, the plane motion of the robot's body along two mutually perpendicular axes is studied. Therefore, the corresponding projections of the inertial forces acting upon the mass m_1 at point *O* (see Fig. 1) can be expressed as follows:

$$F_{in.x} = -m_1 \cdot \ddot{x}_1; \quad F_{in.y} = -m_1 \cdot \ddot{y}_1, \tag{1}$$

where $\ddot{x}_1$, $\ddot{y}_1$ denote the second-order time derivatives of the corresponding displacements x_1, y_1.

Let us present the angles φ_1, φ_2 (see Fig. 1) as the functions of the generalized coordinates x_1, y_1:

$$\varphi_1 = \arctan\left(\frac{L_{DB.0} \cdot \sin\varphi_{1.0} + y_1}{L_{DB.0} \cdot \cos\varphi_{1.0} + x_1}\right); \tag{2}$$

$$\varphi_2 = \arctan\left(\frac{L_{DB.0} \cdot \sin\varphi_{1.0} + y_1}{\frac{L_{DB.0} \cdot \sin\varphi_{1.0}}{\tan(\varphi_{2.0})} - x_1}\right), \tag{3}$$

where $L_{DB.0}$ is the initial length of the spring-damper member D_1B_1 in the robot's suspension equilibrium position (in the state of rest); $\varphi_{1.0}$ is the initial angle between the straight line connecting the hinges D_1, B_1 and the positive direction of the horizontal axis *Ox*; $\varphi_{2.0}$ is the initial angle between the straight line connecting the hinges D_1, A_1 and the negative direction of the horizontal axis *Ox*.

The dependencies of the lengths of the spring-damper members D_1B_1 and D_1A_1 on the displacements x_1, y_1 can be written as follows:

$$L_{DB} = \sqrt{\left(L_{DB.0} \cdot \cos\varphi_{1.0} + x_1\right)^2 + \left(L_{DB.0} \cdot \sin\varphi_{1.0} + y_1\right)^2}; \tag{4}$$

$$\Delta L_{DB} = L_{DB.0} - L_{DB} = L_{DB.0} - \sqrt{\left(L_{DB.0} \cdot \cos\varphi_{1.0} + x_1\right)^2 + \left(L_{DB.0} \cdot \sin\varphi_{1.0} + y_1\right)^2}; \tag{5}$$

$$L_{DA} = \sqrt{\left(\frac{L_{DB.0} \cdot \sin\varphi_{1.0}}{\tan(\varphi_{2.0})} - x_1\right)^2 + \left(L_{DB.0} \cdot \sin\varphi_{1.0} + y_1\right)^2}; \tag{6}$$

$$\Delta L_{DA} = L_{DA.0} - L_{DA} = \frac{L_{DB.0} \cdot \sin\varphi_{1.0}}{\sin(\varphi_{2.0})} - \sqrt{\left(\frac{L_{DB.0} \cdot \sin\varphi_{1.0}}{\tan(\varphi_{2.0})} - x_1\right)^2 + \left(L_{DB.0} \cdot \sin\varphi_{1.0} + y_1\right)^2}. \tag{7}$$

The suspension acts upon the robot's body in vertical direction only in the case when its vertical displacement is less than the static deflection y_{st} caused by the gravity forces, i.e., when the robot moves under the non-detachable (non-jumping) conditions. Otherwise, the suspension vertical action is equal to zero. The suspension system spring force acts upon the robot's body in horizontal direction only in the case when its absolute horizontal value is less than the absolute value of the friction force F_{fr} acting between the supporting feet and the rough surface. Otherwise, the suspension horizontal action is equal to the friction

force F_{fr}. Similar conclusions can be drawn about the suspension damping forces. Therefore, let us derive the simplified expressions of the corresponding projections of the spring and damping forces:

$$F_{spr.x} = \begin{cases} -k_1 \cdot \Delta L_{DA} \cdot \cos\varphi_2 + k_2 \cdot \Delta L_{DB} \cdot \cos\varphi_1, & \text{if } \left|-k_1 \cdot \Delta L_{DA} \cdot \cos\varphi_2 + k_2 \cdot \Delta L_{DB} \cdot \cos\varphi_1\right| \le \left|F_{fr}\right|; \\ F_{fr}, & \text{if } \left|-k_1 \cdot \Delta L_{DA} \cdot \cos\varphi_2 + k_2 \cdot \Delta L_{DB} \cdot \cos\varphi_1\right| > \left|F_{fr}\right|; \end{cases} \tag{8}$$

$$F_{spr.y} = \begin{cases} k_1 \cdot \Delta L_{DA} \cdot \sin\varphi_2 + k_2 \cdot \Delta L_{DB} \cdot \sin\varphi_1, & \text{if } y_1 \le y_{st}; \\ 0 & \text{if } y_1 > y_{st}; \end{cases} \tag{9}$$

$$F_{dam.x} = \begin{cases} -c_1 \cdot \Delta \dot{L}_{DA} \cdot \cos\varphi_2 + c_2 \cdot \Delta \dot{L}_{DB} \cdot \cos\varphi_1, & \text{if } \left|-k_1 \cdot \Delta L_{DA} \cdot \cos\varphi_2 + k_2 \cdot \Delta L_{DB} \cdot \cos\varphi_1\right| \le \left|F_{fr}\right|; \\ 0, & \text{if } \left|-k_1 \cdot \Delta L_{DA} \cdot \cos\varphi_2 + k_2 \cdot \Delta L_{DB} \cdot \cos\varphi_1\right| > \left|F_{fr}\right|; \end{cases} \tag{10}$$

$$F_{dam.y} = \begin{cases} c_1 \cdot \Delta \dot{L}_{DA} \cdot \sin\varphi_2 + c_2 \cdot \Delta \dot{L}_{DB} \cdot \sin\varphi_1, & \text{if } y_1 \le y_{st}; \\ 0 & \text{if } y_1 > y_{st}, \end{cases} \tag{11}$$

where $\Delta \dot{L}_{DA}$, $\Delta \dot{L}_{DB}$ denote the first-order time derivatives of the corresponding displacements ΔL_{DA}, ΔL_{DB}; y_{st} is the suspension vertical static deflection caused by the gravity forces acting upon the robot's body in its equilibrium position (in the state of rest).

The dry friction force acting between the supporting feet and the rough surface, along which the robot is sliding, can be approximately determined as follows:

$$F_{fr} = \begin{cases} -\left(m_1 \cdot g - F_{spr.y} - F_{dam.y}\right) \cdot \mu_{fr.k} \cdot \operatorname{sign}\left(\dot{x}_1\right), & \text{if } y_1 \le y_{st} \wedge \dot{x}_1 \ne 0; \\ -\left(m_1 \cdot g - F_{spr.y} - F_{dam.y}\right) \cdot \mu_{fr.s} \cdot \operatorname{sign}\left(x_1\right), & \text{if } y_1 \le y_{st} \wedge \dot{x}_1 = 0; \\ 0 & \text{if } y_1 > y_{st}, \end{cases} \tag{12}$$

where g is the free-fall (gravity) acceleration; $\dot{x}_1$ denotes the first-order time derivatives of the robot's body horizontal displacement; $\operatorname{sign}\left(\dot{x}_1\right)$ is the function defining the direction of the robot's body motion; $\operatorname{sign}\left(x_1\right)$ is the function defining the horizontal position of the position.

The suspension vertical static deflection y_{st} caused by the gravity forces acting upon the robot's body in its state of rest can be derived from the corresponding equilibrium conditions:

$$\begin{gathered} m_1 \cdot g - F_{spr.y} = 0 \underset{y_1 \to y_{st}}{\Rightarrow} k_1 \cdot \Delta L_{DA} \cdot \sin\varphi_2 + k_2 \cdot \Delta L_{DB} \cdot \sin\varphi_1 = m_1 \cdot g. \\ F_{spr.x} = 0 \underset{y_1 \to y_{st}}{\Rightarrow} -k_1 \cdot \Delta L_{DA} \cdot \cos\varphi_2 + k_2 \cdot \Delta L_{DB} \cdot \cos\varphi_1 = 0. \end{gathered} \tag{13}$$

Substitution of equations (2), (3), (5), (7) into the equilibrium conditions (13) leads to the extra-large analytical expression for y_{st}. In our case, let us consider the small-amplitude oscillations of the robot's body with respect to the suspension's overall dimensions. This allows for assuming the angles φ_1, φ_2 to be constant and for simplifying the analytical expression for y_{st}:

$$y_{st} \approx \frac{m_1 \cdot g}{k_1 \cdot \sin\varphi_{20} + k_2 \cdot \sin\varphi_{10}}. \tag{14}$$

Taking into account the derived expressions (1)–(14), the mathematical model describing the robot motion can be presented as the system of two differential equations:

$$F_{in.x} + F_{spr.x} + F_{dam.x} + F_{1x} = 0; \tag{15}$$

$$F_{in.y} + F_{spr.y} + F_{dam.y} + F_{1y} = 0. \tag{16}$$

Due to the extra-large analytical form of the equations (15), (16), let us omit their full presentation in the present paper. The following stages of the carried out investigation are dedicated to the numerical modeling and computer simulation of the system motion. The input data to be predefined is following: the

initial geometric, stiffness, and damping parameters of the suspension ($L_{DB.0}$, $\varphi_{1.0}$, $\varphi_{2.0}$, k_1, k_2, c_1, c_2); the robot's body mass (m_1); friction parameters ($\mu_{fr.s}$, $\mu_{fr.k}$); excitation forces (F_{1x}, F_{1y}).

Results and Discussion

Numerical modeling of the robot motion in the Mathematica software.

In order to carry out further numerical modeling and computer simulation, let us introduce the robot's parameters: $m_1 = 30$ kg, $k_1 = 0$ N/m, $k_2 = 3 \cdot 10^4$ N/m, $c_1 = 0$ N·s/m, $c_2 = 50$ N·s/m, $\mu_{fr.k} = 0.5$, $\mu_{fr.s} = 0.6$, $F_{1x} = 100 \cdot \sin(30 \cdot t)$ N, $F_{1y} = 100 \cdot \sin(30 \cdot t)$ N, $L_{DB.0} = 0.2$ m, $\varphi_{10} = \pi/4$, $\varphi_{20} = \pi/2$. In the considered case, the robot's body performs the straight-line (directed) oscillations at the angle of approximately 45° with a horizontal axis and simultaneously slides along the rough horizontal surface (see Figs. 2 and 3). Fig. 2 presents time dependencies of the robot's body horizontal and vertical displacements, speeds, and accelerations, while Fig 3 shows the trajectory (path) of its mass center motion.

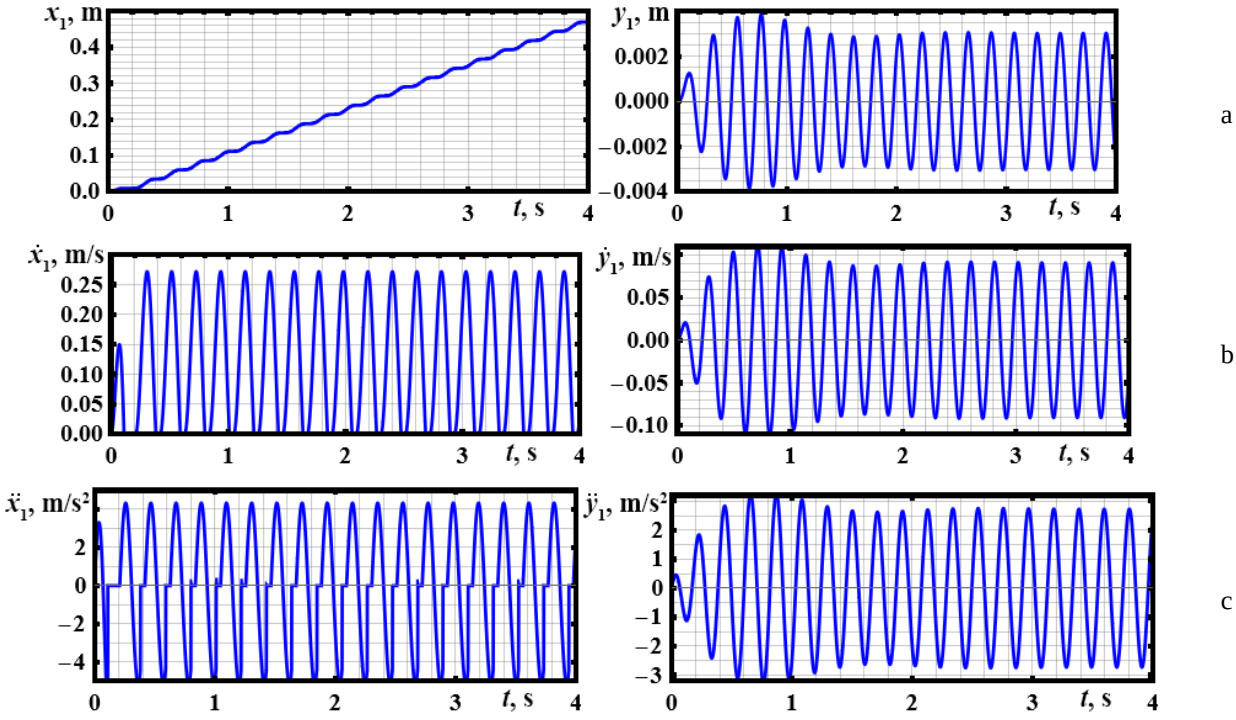

Fig. 2. Time dependencies of the robot's mass center horizontal and vertical displacements (a), velocities (b) and accelerations (c) obtained by numerical modeling in the Mathematica software

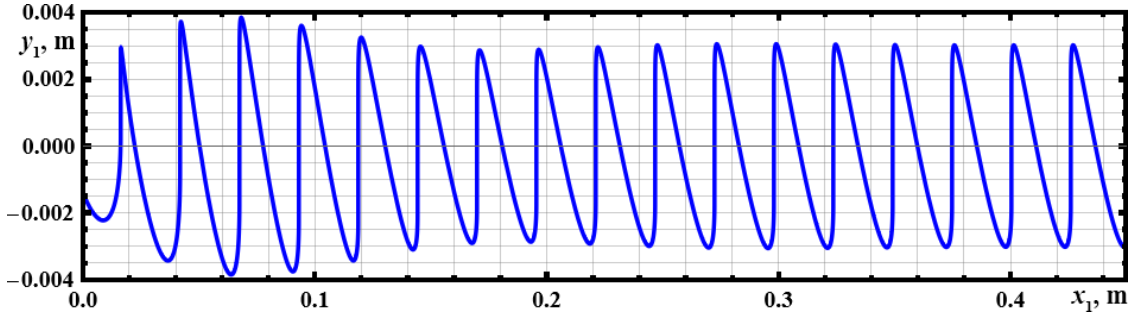

Fig. 3. Motion path of the robot's mass center obtained by numerical modeling in the Mathematica software

The maximal vertical displacement of the robot's body from its equilibrium position is about 3 mm, while the maximal horizontal displacement during one step (period) reaches 26 mm. The maximal

horizontal and vertical speeds are 0.27 m/s, 0.058 m/s, respectively. The robot's average locomotion speed is about 0.11 m/s. The amplitude values of vertical and horizontal accelerations reach 4.4 m/s^2, 2.75 m/s^2, respectively. The results of numerical modeling show that the maximal vertical acceleration of the robot's body doesn't exceed the free-fall (gravity) acceleration. This allows for drawing the conclusion about the nondetachable motion conditions (no bouncing, jumping, or skipping over the horizontal surface). Let us analyze the correctness of the derived mathematical model describing the robot motion by means of the computer simulation of the robot's suspension operation in the MapleSim and SolidWorks software.

Simulation of the robot's suspension in the MapleSim software.

Fig. 4 presents the simulation model of the robot's suspension developed in the MapleSim software according to the dynamic diagram considered above. The prismatic sliders P_2, P_6 are sliding along the horizontal axis whose origins are located at the fixed frames FF_1, FF_2. Four rigid body frames (rods) RBF_1, RBF , RBF_5, RBF_7 are fixed to the movable ends of the sliders P_2, P_6. The spring-damper elements SD_1, SD_2, SD_3, SD_4 control the prismatic sliders P_1, P_3, P_4, P_5 displacements. The later are hinged to the rods RBF_1, RBF_2, RBF_3, RBF_4, RBF_5, RBF_6, RBF_7, RBF_8 by the revolute joints R_2, R_3, R_4, R_1, R_6, R_5, R_8, R_7, respectively. The rigid bodies RB_1, RB_2, RB_3 are located between the rods RBF_9-RBF_{10}, RBF_3-RBF_4, RBF_8-RBF_6 of the same lengths. The body RB_1 is subjected to the action of the disturbing periodical forces simulated by the Applied World Force AWF_1 block and sinusoidal signal blocks S_1, S_2 defining its horizontal and vertical components. The friction forces are applied between the ends of the sliders P_2, P_6 and are simulated by the friction brakes B_1, B_2. The magnitudes of the normal forces acting upon the braking blocks are defined by the Force-and-Moment Sensors FAM_1, FAM_2. The vertical components of the forces acting upon the sliding blocks and defining the magnitudes of the normal braking forces are determined by analyzing the sensors FAM_1, FAM_2 signals using the real demultiplexers DMR_1, DMR_2.

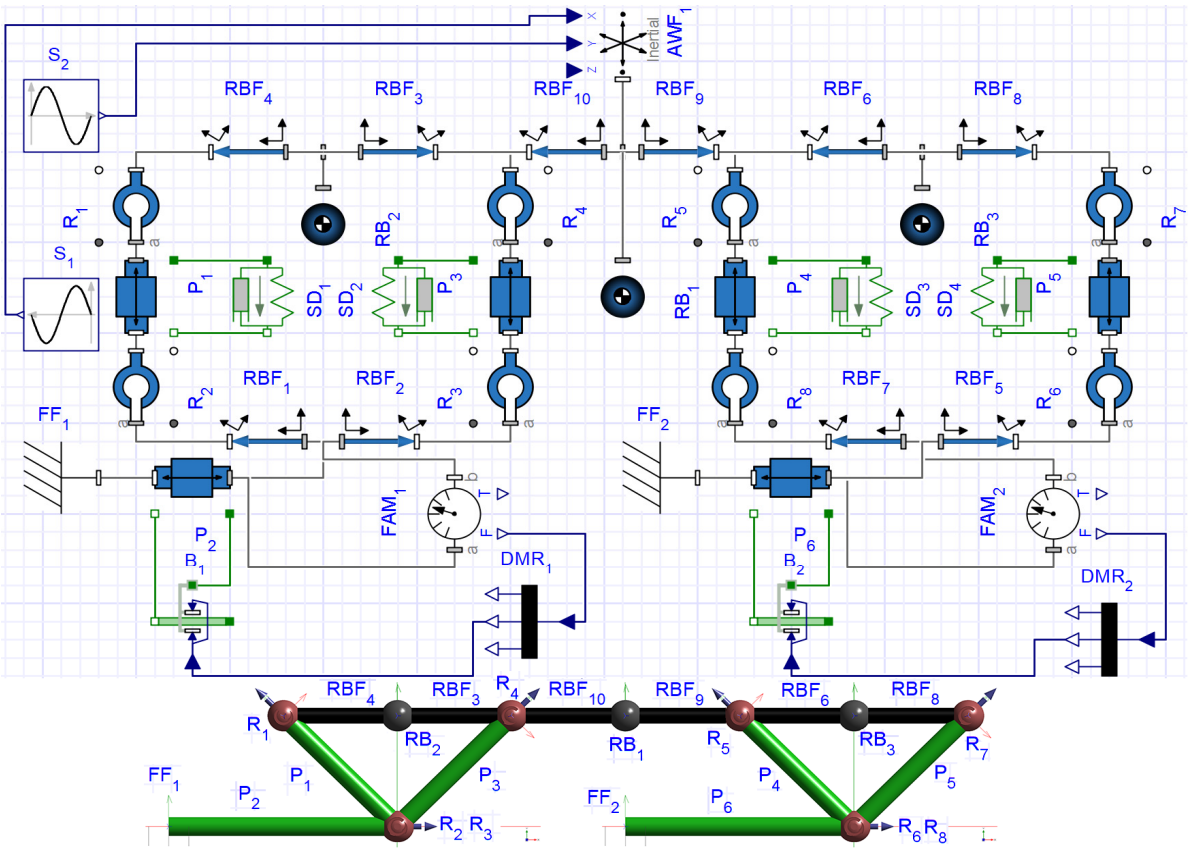

Fig. 4. Simulation model of the robot's suspension developed in MapleSim software

Prescribing the same input parameters of the robot's suspension as in the previous section dedicated to the numerical modeling, the corresponding simulation results have been obtained (see Fig. 5). The robot's body has passed about 0.45 m during the first 4 s after the start. Therefore, the average horizontal speed exceeds 0.1 m/s. The vertical oscillations amplitude is approximately 0.003 m. The general character of the robot motion simulated in the MapleSim software satisfactorily agrees with the results of numerical modeling carried out in the Mathematica software. The minor differences can be observed on the path

(trajectory) plots of the robot's mass center (see Fig. 3 and Fig. 5, *b*). This fact can be explained by the phase shifts of the horizontal and vertical components of the disturbing forces and the difference between the initial conditions applied in numerical modeling and computer simulation. Therefore, let us omit the plots of the rest kinematic parameters, in particular, the velocities and accelerations of the robot's body.

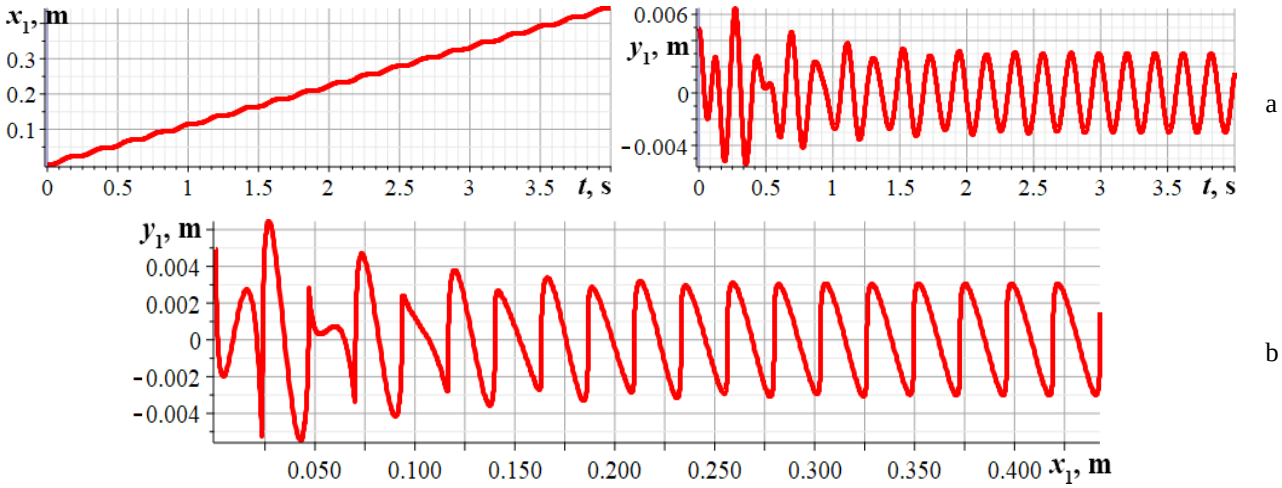

Fig. 5. Time dependencies of the robot's mass center horizontal and vertical displacements (a) and its motion path (b) simulated in the MapleSim software

Computer modeling of the robot motion in the SolidWorks software.

The next stage of the present study aimed at analyzing the correctness of the derived mathematical model consists in computer simulation of the robot motion in the SolidWorks software. The corresponding suspension model is presented in Fig. 6. It consists of the horizontal unmovable plate 4, feet 3, suspension system 2 and the rigid movable plate 1. The coincidence contact between the corresponding surfaces of the bodies 3 and 4 is characterized by the sliding friction coefficients $\mu_{fr.s}$, $\mu_{fr.k}$. The gravity force acts vertically downwards. All the geometrical, inertial, stiffness, and damping parameters correspond to the ones used in the previous sections of the paper. The active (disturbing) forces F_{1x}, F_{1y} are applied to the mass center m_1 of the robot's body (movable plate 1). All the hinges A_1, A_2, B_1, B_2, D_1, D_{12} are simulated as the ideal revolute joints (with no friction and clearance). The springs (colored in red) are characterized by the linear exponents of the spring and damper forces expressions with the corresponding coefficients k_1, k_2, c_1, c_2.

The results of computer modeling of the robot motion are presented in Fig. 7. In analogy to the previous simulation, let us analyze time dependencies of the robot's body horizontal and vertical displacements (Fig. 7, *a*), and its motion path (Fig. 7, *b*). Due to some inconveniences of starting the robot's body motion from the zero-position, the plots have a little bit different scale (starting and end points). Nevertheless, it can be concluded that the horizontal locomotion speed exceeds 100 mm/s, the amplitude of the robot's body vertical oscillations is about 3 mm, and the general character of the

robot motion is approximately the same as the ones simulated above. Therefore, the conclusion about the correctness of the derived mathematical model describing the robot motion can be drawn. While performing further investigations on the subject of the paper, it is expedient to the substantiate the robot's inertial, stiffness, damping, and excitation parameters with the purpose of maximizing the robot's locomotion velocity.

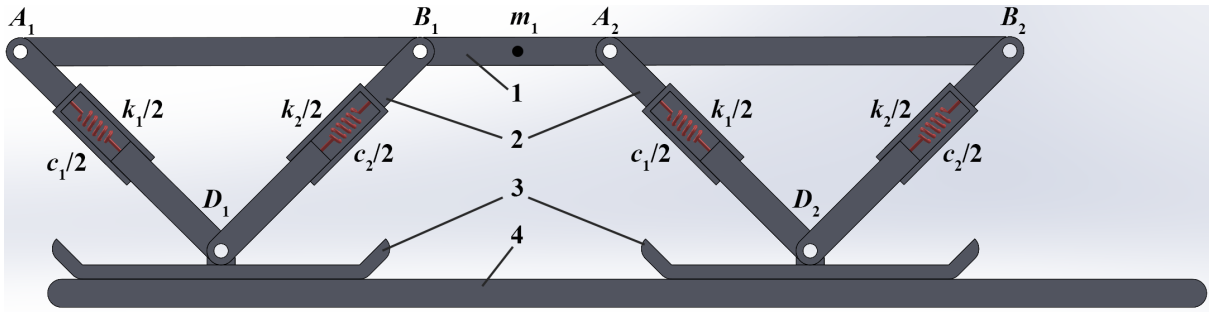

Fig. 6. Simulation model of the robot's suspension developed in SolidWorks software

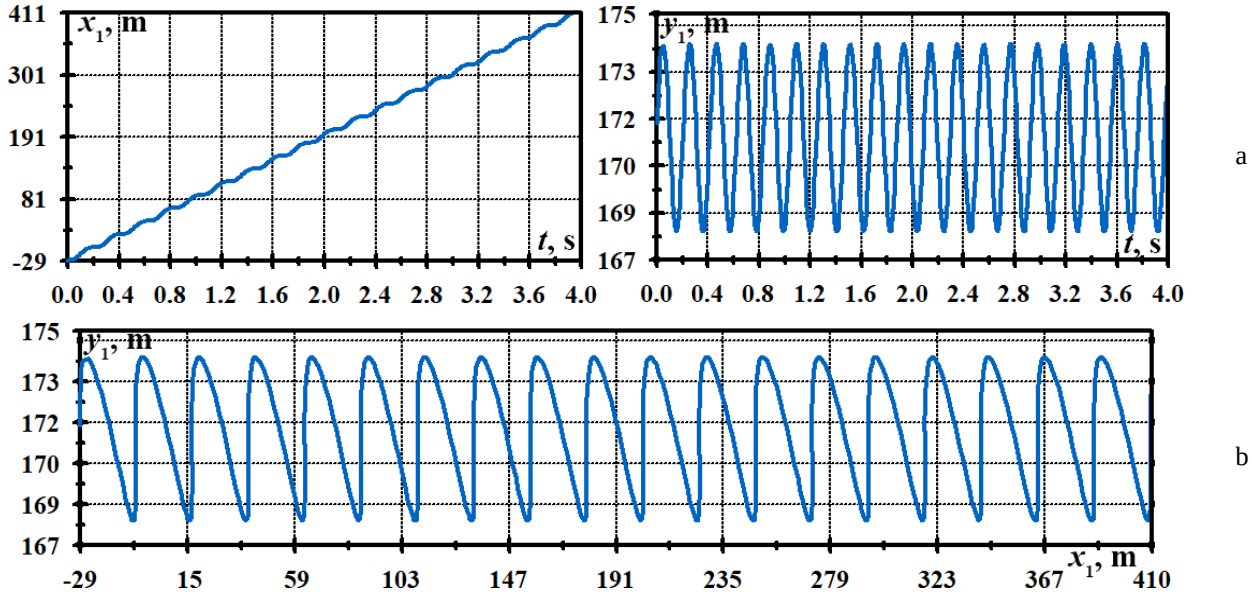

Fig. 7. Time dependencies of the robot's mass center horizontal and vertical displacements (a) and its motion path (b) simulated in the SolidWorks software

Conclusions

Based on the thorough analysis of various research publications dedicated to the vibration-driven robots and their locomotion principles, the present paper considers the generalized dynamic diagram of the robot's combined four-spring suspension system (Fig. 1). The corresponding mathematical model describing the robot locomotion is developed using the Lagrange-d'Alembert principle. The numerical modeling of the robot motion during the first 4 s after the start is carried out in the Mathematica software by solving the derived system of differential equations with the help of the Runge-Kutta methods.

The maximal vertical displacement of the robot's body from its equilibrium position is about 3 mm, while the maximal horizontal displacement during one step (period) reaches 26 mm. The maximal horizontal and vertical speeds are 0.27 m/s, 0.058 m/s, respectively. The robot's average locomotion speed is about 0.11 m/s. The amplitude values of vertical and horizontal accelerations

reach 4.4 m/s^2, 2.75 m/s^2, respectively. The results of numerical modeling show that the maximal vertical acceleration of the robot's body doesn't exceed the free-fall (gravity) acceleration. This allows for drawing the conclusion about the nondetachable motion conditions (no bouncing, jumping, or skipping over the horizontal surface).

In order to verify the correctness of the derived mathematical model describing the robot motion, the corresponding computer simulation is carried out in the MapleSim and SolidWorks software. The simplified models of the robot's suspension are presented in Figs. 4 and 6. The computer simulation results (Figs. 5 and 7) satisfactorily agree with the results of numerical modeling carried out in the Mathematica software. While performing further investigations on the subject of the paper, it is expedient to the substantiate the robot's inertial, stiffness, damping, and excitation parameters with the purpose of maximizing the robot's locomotion velocity and minimizing the energy consumption.

References

[1] L. Jaulin, *Mobile Robotics*, 2nd ed. Hoboken, NJ, USA: John Wiley & Sons, Inc., 2019. https://doi.org/10.1002/9781119663546.

[2] N. Bolotnik, I. Zeidis, K. Zimmermann, and S. Yatsun, "Vibration driven robots", in *Proc. 56th International Scientific Colloquium "Innovation in Mechanical Engineering – Shaping the Future"*, Ilmenau University of Technology, Ilmenau, Germany, September 12–16, 2011, pp. 1–6.

[3] Y. Yan, Y. Liu, J. Páez Chávez, F. Zonta, and A. Yusupov, "Proof-of-concept prototype development of the self-propelled capsule system for pipeline inspection," *Meccanica*, vol. 53, no. 8, pp. 1997–2012, Jun. 2018. https://doi.org/10.1007/S11012-017-0801-3.

[4] I. Loukanov, V. Vitliemov, S. Stoyanov, and S. Stoyanov, "Design developments of vibration-driven robots," in *Proc. 56th Science Conference of Ruse University*, Ruse, Bulgaria, 2017, pp. 50–59.

[5] R. M. Morariu-Gligor, A. V. Crişan, and F. M. Şerdean, "Optimal design of an one-way plate compactor," *ACTA TECHNICA NAPOCENSIS*, vol. 60, no. 4, pp. 557–564, Nov. 2017.

[6] L. Crisóstomo, N. F. Ferreira, and V. Filipe, "Robotics services at home support," *International Journal of Advanced Robotic Systems*, vol. 17, no. 4, pp. 1–11, 2020. https://doi.org/10.1177/1729881420925018

[7] K. Ragulskis et al., "Investigation of dynamics of a pipe robot with vibrational drive and unsymmetric with respect to the direction of velocity of motion dissipative forces," *Agricultural Engineering*, vol. 52, pp. 1–6, 2020. https://doi.org/10.15544/ageng.2020.52.1.

[8] Y. Yan, Y. Liu, L. Manfredi, and S. Prasad, "Modelling of a vibro-impact self-propelled capsule in the small intestine," *Nonlinear Dynamics*, vol. 96, no. 1, pp. 123–144, 2019. https://doi.org/10.1007/s11071-019-04779-z

[9] B. Guo, Y. Liu, R. Birler, and S. Prasad, "Self-propelled capsule endoscopy for small-bowel examination: Proof-of-concept and model verification," *International Journal of Mechanical Sciences*, vol. 174, Article ID 105506, 2020. https://doi.org/10.1016/j.ijmecsci.2020.105506.

[10] V. Korendiy, "Substantiation of parameters and motion modelling of two-mass mobile vibratory system with two unbalanced vibration exciters," *Avtomatizaciâ virobničih procesìv u mašinobuduvannì ta priladobuduvannì*, vol. 52, pp. 16–31, 2018. https://doi.org/10.23939/istcipa2018.52.016.

[11] M. Schulke, L. Hartmann, and C. Behn, "Worm-like locomotion systems: development of drives and selective anisotropic friction structures," in *Proc. 56th International Scientific Colloquium "Innovation in Mechanical Engineering – Shaping the Future"*, Ilmenau, Germany, September 12–16, 2011, pp. 1–21.

[12] V. Korendiy, "Dynamics of two-mass mobile vibratory robot with electromagnetic drive and vibro-impact operation mode," *Ukrainian Journal of Mechanical Engineering and Materials Science*, vol. 4, no. 2, pp. 80–93, 2018. https://doi.org/10.23939/ujmems2018.02.080.

[13] V. Du Nguyen and N. T. La, "An improvement of vibration-driven locomotion module for capsule robots," *Mechanics Based Design of Structures and Machines*, vol. 49, no. 7, pp. 1–15, 2020. https://doi.org/10.1080/15397734.2020.1760880.

[14] O. Lanets, O. Kachur, V. Korendiy, and V. Lozynskyy, "Controllable crank mechanism for exciting oscillations of vibratory equipment," in *Lecture Notes in Mechanical Engineering*, pp. 43–52, 2021. https://doi.org/10.1007/978-3-030-77823-1_5.

[15] V. Korendiy, V. Gursky, O. Kachur, V. Gurey, O. Havrylchenko, and O. Kotsiumbas, “Mathematical modeling of forced oscillations of semidefinite vibro-impact system sliding along rough horizontal surface,” *Vibroengineering Procedia*, vol. 39, pp. 164–169, 2021. https://doi.org/10.21595/vp.2021.22298.

[16] G. Cicconofri, F. Becker, G. Noselli, A. Desimone, and K. Zimmermann, “The inversion of motion of Bristle Bots: analytical and experimental analysis,” in *Parenti-Castelli V., Schiehlen W. (eds), ROMANSY 21 – Robot Design, Dynamics and Control. CISM International Centre for Mechanical Sciences (Courses and Lectures)*, vol. 569, Springer, Cham., 2016, pp. 225–232. https://doi.org/10.1007/978-3-319-33714-2_25.

[17] D. Kim, Z. Hao, A. R. Mohazab, and A. Ansari, “On the forward and backward motion of milli-bristle-bots,” *International Journal of Non-Linear Mechanics*, vol. 127, Article ID 103551, 2020. https://doi.org/10.1016/j.ijnonlinmec.2020.103551.

[18] D. W. Choi, C. W. Lee, D. Y. Lee, D. W. Lee, and H. U. Yoon, “A hybrid soft actuator inspired by grass-spike: Design approach, dynamic model, and applications,” *Applied Sciences (Switzerland)*, vol. 10, no. 23, pp. 1–15, 2020. https://doi.org/10.3390/app10238525.

[19] C. Hastings, K. Mischo, and M. Morrison, *Hands-on Start to Wolfram Mathematica and Programming with the Wolfram Language*, 2nd ed. Champaign, IL, USA: Wolfram Media, Inc., 2016.

[20] R. Müller, *Modellierung, Analyse und Simulation Elektrischer und Mechanischer Systeme mit Maple und MapleSim [Modeling, Analysis and Simulation of Electrical and Mechanical Systems with Maple and MapleSim]*, 2nd ed. Wiesbaden, Germany: Springer Vieweg, 2020, (in German). https://doi.org/10.1007/978-3-658-29131-0.

[21] K.-H. Chang, *Motion Simulation and Mechanism Design with SOLIDWORKS Motion 2021*. Mission, KS, USA: SDC Publications, 2021.